An Integrated Early Warning System for Stock Market Turbulence

Peiwan Wang[a,b], Lu Zong[a,b,*], Ye Ma[a,b]

[a]*Department of Mathematical Sciences, Xi'an Jiaotong-Liverpool University.*
[b]*111 Ren'ai Road, Dushu Lake Science and Education Innovation District, Suzhou Industrial Park, Suzhou, Jiangsu Province, P.R. China, 215123.*

Abstract

This study constructs an integrated early warning system (EWS) that identifies and predicts stock market turbulence. Based on switching ARCH (SWARCH) filtering probabilities of the high volatility regime, the proposed EWS first classifies stock market crises according to an indicator function with thresholds dynamically selected by the two-peak method. An hybrid algorithm is then developed in the framework of a long short-term memory (LSTM) network to make daily predictions that alert turmoils. In the empirical evaluation based on ten-year Chinese stock data, the proposed EWS yields satisfying results with the test-set accuracy of 96.6% and on average 2.4 days of forewarned period. The model's stability and practical value in the real-time decision-making are also proven by the cross-validation and back-testing.

Keywords: Early warning system, LSTM, SWARCH, two-peak method, dynamic prediction

1. Introduction

Due to the Subprime Mortgage crisis, the Shanghai Stock Exchange Composite (SSEC) index experienced one of its greatest falls in the end of 2007. In mid-2015, another Chinese stock market bubble crashed and led to extreme turbulence and instability in the domestic financial environment. As the lasting effect of stock market crises is recognized as the cause of critical society stress and results in increasing financial loads of the government, a systematic model that monitors the economic scenarios of financial markets, and generates early warning signals for potential extreme risks is in heavy demand.

Financial early warning systems (EWSs) are designed to forecast crises via studying pre-turmoil patterns, thus to allow market participants to take early actions to hedge against vital risks. In practice, the target of early warning ranges from individual financial markets, such as the banking sector, the currency and stock markets, to the entire

---

economic system. The modeling of crises are then commonly formulated as a classification problem based on the identified crisis indicators. To design an effective and reliable EWS with true warnings and limited false alarms, two matters need to be delicately addressed, that is the identification of crises and the mechanism of prediction.

In the previous studies, an EWS is primarily constructed by identifying crises on the basis of either expert opinions or an indicator function describing the market crash. The former approach is widely used in the early studies of EWS, especially those concerning banking and debt crises (Kaminsky and Reinhart, 1999; Kaminsky, 2006; Reinhart and Rogoff, 2011, 2013; Caprio and Klingebiel, 2002; Valencia and Laeven, 2008; Laeven and Valencia, 2010, 2012; Detragiache and Spilimbergo, 2001; Yeyati and Panizza, 2011). Despite that the expert-defined crises are considered to be reliable for long-term predictions (Oh et al., 2006), this paradigm fails to offer an efficient modeling solution as the frequency of observation increases. On the other hand, indicator functions based on a pre-specified threshold are more frequently used to define currency or stock market crashes. Reinhart and Rogoff (2011) define a currency crisis as the excessive exchange rate depreciation exceeds the threshold value of 15%. Alternatively, Eichengreen et al. (1995) propose to use the Financial Pressure Index (FPI) to measure the gross foreign exchange reserves of the Central Bank and the repo rate (Sevim et al., 2014). Currency crises are thus identified as the FPI raises more than 1.5 (Kibritcioglu et al., 1999), 2 (Eichengreen et al., 1995; Bussiere and Fratzscher, 2006), 2.5 (Edison, 2003) or, 3 (Kaminsky and Reinhart, 1999; Berg and Pattillo, 1999; Duan and Bajona, 2008)) standard deviations from its long-term mean. In the context of stock EWS, market crashes are indicated by the CMAX index falling below its mean by 2 (Coudert and Gex, 2008), 2.5 (Li et al., 2015), or 3 (Fu et al., 2019) standard deviations. In terms of expressing crises as indicator functions, two major drawbacks emerge in the practical aspect. Despite that the paradigm of handling crises as crashes captures the associated acute loss, it fails to consider the extreme risk that comes along with the volatility jump. Moreover, the selection of crisis thresholds should be handled more delicately taking into account the trade-off between missing crises and false alarms resulted from over-/under-estimated thresholds (Babecký et al., 2014).

In terms of the predictive model, three types of methods are commonly applied to generate early warning signals for currency, banking and debt crises, namely the logit-probit regression (Frankel and Rose, 1996; Eichengreen and Rose, 1998; Demirg-Kunt and Detragiache, 1998; Bussiere and Fratzscher, 2006; Beckmann, 2007) , the signaling approach (Kaminsky and Reinhart, 1999; Kaminsky, 1998; Berg and Pattillo, 1999; Davis and Karim, 2008) and machine learning-based models (Nag and Mitra, 1999; Kim et al., 2004a; Celik and Karatepe, 2007; Yu et al., 2010; Giovanis, 2012; Sevim et al., 2014). Among the limited studies on stock markets (Fu et al., 2019), Coudert and Gex (2008) use logit and multi-logit models to predict stock and currency crises and find the leading effect of risk aversion indicators for stock early warning. Li et al. (2015) shows the significance of S&P 500 futures and options in predicting stock crashes basing on a logit model. By combining the logit model and Ensemble Empirical Mode Decomposition, (Fu et al., 2019) recently develop an EWS for daily stock crashes using investor sentiment indicators and achieve good in-sample and test-set results. Due to the non-linear nature of financial data, machine-learning algorithms are also recognized tools in the general field of stock market prediction. In the literature of EWS, artificial neural networks (Kim et al., 2004a; Oh et al., 2006; Kim et al., 2004b; Yu et al., 2010; Sevim et al., 2014;

Celik and Karatepe, 2007), fuzzy inference (Lin and Khan, 2008; Nan and Zhou, 2012; Giovanis, 2012; Fang, 2012) and support vector machines (SVM) (Hui and Wang; Hu and Pang, 2008; Ahn et al., 2011) are proven accurate models for financial crisis prediction. Despite the promising accuracy demonstrated by those studies, few investigates the test-set early warning power of the model, that is the duration of forewarned period before the crisis onset.

To fill in the gaps discussed above, the objectives of this study are threefold. First, we attempt to develop a robust crisis classifier to precisely identify stock market turbulence on daily basis. The crisis classifier consists of two key components, namely the switching ARCH (SWARCH) model (Hamilton and Susmel, 1994) and two-peak (or valley-of-two-peaks) method (Rosenfeld and De La Torre, 1983). Instead of focusing on the return horizon, the proposed classifier tackles the problem from the perspective of the volatility (Rodriguez, 2007; Kim, 2013; Fink et al., 2016; BenSaïda, 2018; BenMim and BenSaïda, 2019). The switching ARCH (SWARCH) model is adopted to label crisis/non-crisis episodes with high/low volatility regimes that imply market turbulence/tranquility (Hamilton and Susmel, 1994; Hamilton and Gang, 1996; Ramchand and Susmel, 1998; Edwards and Susmel, 2001). The model's effectiveness in depicting Chinese stock crises is explicitly examined in the authors' previous study on the contagion effect among housing, stock, interest rate and currency markets in China and the U.S. (Wang and Zong, 2019). On the other hand, the two-peak method is an automatic thresholding approach (Jain et al., 1995) which selects classification thresholds automatically based on pre-determined principles in order to obtain more robust segmentation. To classify stock turbulence, the two-peak method is performed on the histogram of SWARCH filtering possibilities to determine the optimal crisis cut-off. Second, a dynamic early warning system is developed integrating the crisis classifier and long short-term memory (LSTM) neural network (Jordan, 1997) to alert crisis onsets. As for the predictive model, LSTM is proven to be a state-of-art mechanism in the general field of financial forecasting (Chen et al., 2015; Fischer and Krauss, 2018; Wu and Gao, 2018; Cao et al., 2019), including volatility forecasting (Yu and Li, 2018; Kim and Won, 2018; Liu, 2019). To the best of the authors' knowledge, this study is the first that incorporates LSTM in an EWS. Last, a comprehensive evaluation of the EWS is conducted by first examining the crisis classifier and predictor separately. To be specific, we empirically study the precision and robustness of the crisis classifier in comparison to the most widely used approach which defines stock crises according to an indicator functions of CMAX. The LSTM crisis predictor is then evaluated upon two baseline models, i.e. the back-propagation neural network (BPNN) and support vector regression (SVR), regarding to the performance metrics including the rand accuacry, binary cross-entropy loss, receiver operating curve (ROC), area under curve (AUC) and the SAR score. To evaluate the effectiveness and stability of the EWS as a whole, the proposed algorithm is performed in not only the test set but also cross-validation and back-testing. According to the evaluation, the integrated EWS achieves the state-of-art performance and warns stock turbulence in the test set with 96.6% accuracy and on average 2.4 days ahead of crisis onsets.

The remaining part of this paper is organized as follows. Section 2 describes the data included. Section 3 explicitly introduces the structure of the EWS and the algorithm related to the dynamic prediction of stock turbulence. Section 4 evaluates the model according to its performance, and Section 5 summarizes the conclusion.

2. Data

Data	Frequency	Reflection	Source
Close price, log returns and realized volatilities of the SSEC index	Daily	Endogenous factors	WIND database
S&P500 Stock Price Index	Daily	US stock market	Yahoo finance
USD/CNY exchange rate	Daily	Currency	US Federal Reserve Board
Gold Price Oil Price	Daily	Global economy	World Gold Council International Monetary Fund
Interest rate for China(IMF published), M1, M2, CPI	Monthly	Domestic economy	WIND database

In this study, the Shanghai Stock Exchange Composite (SSEC) index is hired to reflect the Chinese stock market oscillation. Explanatory variables that are incorporated to predict stock crises are described in Table 1 in terms of frequency, purpose and source. Specifically, endogenous factors include the close price, log return and realized volatility[1] of the SSEC index. The rest of the variables are exogenous factors of four genres reflecting the U.S. stock market, currency level, global and domestic economies, respectively. The samples span from Dec 27, 1998 to Oct 7, 2018 and are split into 70% training and 30% test sets. Table 2 shows the full sample statistics of the explanatory variables.

3. An integrated early warning model

3.1. Crisis identification with SWARCH and two-peak method

3.1.1. High/low volatility regimes in the stock oscillation

Stock crashes are inevitable results of volatility jumps. To explain this phenomenon, we propose to investigate the high/low volatility regime of the stock return based on the SWARCH model (Hamilton and Susmel, 1994). The target is to provide a reliable solution to crisis warning from the perspective of risk.

---

[1]The realized volatility at time t is defined as $\sigma_{rv} = \sqrt{\frac{1}{N_t}\sum_{t=1}^{N_t}(p_t - \bar{p}_t)}$, where the N_t is the count of days after time t, p_t is the log return at t and $\bar{p}_t$ is the average of log return til t.

Table 2: Statistics of explanatory variables. St.Dev. is the standard deviation. $***$ and $**$ denote the (null normal) hypothesis test at the 1% and 5% significance level. † denotes the unit of M1 and M2 is 10^{13} Chinese yuan.

	Mean	St.Dev.	Skewness	Kurtosis	Jarque-Bera
SSEC Close Price	2766.65	560.77	0.68	1.01	291.46***
SSEC log return	0.02	1.49	-0.78	4.86	2643.2***
SSEC realized volatility	1.7	0.31	1.86	4.05	3069.1***
S&P500 Index	1682.81	529.84	0.19	-1.04	124.03***
USD/CNY exchange rate	6.49	0.27	0.06	-1.46	217.38***
Gold Price	1296.08	231.33	0.24	-0.14	26.129***
Oil Price	73.25	22.88	-0.12	-1.41	208.00***
Interest rate for China	3.06	0.22	0.73	2.22	717.48**
M1	3.38†	1.08†	0.47	-0.79	151.87***
M2	1.10†	3.91†	0.12	-1.21	154.91***
CPI	95.83	6.78	-0.4	-1.04	174.59***

Following Hamilton and Susmel (1994), the log return of stock price with high/low volatility regimes could be formulated as a AR(1)-SWARCH(2,1) process given by:

$$y_t = u + \theta_1 y_{t-1} + \epsilon_t, \quad \epsilon_t | \mathcal{I}_{t-1} \sim N(0, h_t); \tag{1}$$

$$\frac{h_t^2}{\gamma_{s_t}} = \alpha_0 + \alpha_1 \frac{\epsilon_{t-1}^2}{\gamma_{s_{t-1}}}, s_t = \{1, 2\}. \tag{2}$$

Eq.(1) describes an AR(1) process with a normal error term ϵ_t of variance h_t. The regime switching structure of the residual variance h_t is given by Eq.(2) where the $\alpha's$ are non-negative, the $\gamma's$ are scaling parameters that capture the change in each regime, s_t is the state variable that $s_t = 1$ indicates the low volatility state, and $s_t = 2$ indicates the high volatility state.

The probability law which results in the stock market switching between the high/low volatility regimes is assumed to be the constant transition probabilities of a two-state Markov chain,

$$p_{ij} = Prob(s_t = j | s_{t-1} = i), i, j = \{1, 2\}. \tag{3}$$

The classification of high/low volatility regimes can be implemented on the basis of the filtering probability, which is a byproduct of the maximum likelihood estimation. The filtering probability based on historical observations till time t, Y_t, written as

$$P(s_t = i | Y_t; \boldsymbol{\theta}_t) \tag{4}$$

where $\boldsymbol{\theta}_t$ is the vector of model parameters to be estimated. Given that $s_t = 2$ is the state of high volatility, $P(s_t = 2 | Y_t; \boldsymbol{\theta}_t)$ can be interpreted as the conditional probability of crises based on the current information of time t. We thus define stock turbulence as the following binary function.

$$\text{Crisis}_t = \begin{cases} 1, & P(s_t = 2 | Y_t; \hat{\boldsymbol{\theta}}_t) \geq c \\ 0, & \text{otherwise.} \end{cases} \tag{5}$$

where $\hat{\boldsymbol{\theta}}_t$ is the estimated parameter vector and c is the crisis threshold/cutoff point.

In this way, stock crisis classification is structured through the mechanism that filtering probabilities of the system being in the high volatility regimes tend to increase as the stock price becomes more volatile, and there exists a threshold c which identifies crises once it is exceeded. By Eq.5, c indicates the lowest-level likelihood of the high-volatility state that could be considered as crises. Hence the determination of c plays a key role in the EWS.

3.1.2. Crisis thresholding: two-peak method

To balance the trade-off between sensitivity and false alarms (Babecký et al., 2014), this study adopts the two-peak method to automatically determine crisis thresholds. The two-peak method is developed with the general purpose of finding the optimal threshold in the context of binary classification, and is proven experimentally credible in solving image processing-related classification problems [2]. According to the two-peak method, the optimal threshold of a binary system is the minimum value between the two peaks of the frequency density histogram (Weszka, 1978). There are several alternative thresholding mechanisms that are built on the histogram, such as the Otsu's method (Ohtsu, 2007) that solves the multi-threshold problem by considering the pixel variance. In this study, we use two-peak as it is the most straightforward of all, and the foundation of other approaches thereafter.

Given that our crisis classifier has two state classes, i.e. crisis (1) and non-crisis (0), the two-peak method is applied to determine the crisis cutoff based on the SWARCH filtering probabilities of the high-volatility state $P(s_t = 2|Y_t; \hat{\boldsymbol{\theta}}_t)$. Specifically, we first sketch the histogram of high-volatility filtering probabilities from time 0 to t. The valley bottom between the two frequency peaks is then selected as the optimal cutoff point at t. To further enhance the robustness of our system, the two-peak method is performed on a recursive basis to obtain dynamic thresholds as the prediction moves forward (See Algorithm 1 in the next section).

3.2. Crisis warning with long-short term memory neural network

The long-short term memory (LSTM) network (Jordan, 1997) belongs to the family of recurrent neural networks (RNNs) (Hochreiter and Schmidhuber, 1997) and is designed to learn both long- and short-term dependencies for sequential forecasting. As a deep learning model, LSTM networks nowadays are widely used in the financial sector in a variety of areas from stock prediction to risk management.

As an extension of classic RNNs, LSTM keeps its merit to allow the processing of sequential data with arbitrary lengths via the hidden state vector, at the same time enhances the learning power of long-distance dependency by introducing the so-called memory cell. As it is displayed in Figure 1, the inputs of a LSTM cell at time t, namely a_{t-1} and C_{t-1}, are memories that contain historical information passed through from the former cell in the form of activation and peephole functions. $\boldsymbol{\Gamma}_f$, $\boldsymbol{\Gamma}_u$, $\boldsymbol{\Gamma}_o$ are sigmoid

---

[2]Prewitt and Mendelsohn (1966) first introduce the two-peak method in the cell image analysis of distinguishing the gray-level difference between the background and the object. The performance of the method is further verified in Rosenfeld and De La Torre (1983) by analyzing the histogram's concavity structure.

functions of the forget gate, the update gate and the output gate that determine the information to be discarded, added and reproduced, respectively. $\tilde{C}_t$ is the new candidate output created by the *tanh* layer, which is limited in the range $[-1, 1]$. Finally, three outputs, $\hat{y}_{t+1}$, a_t and C_t, are produced for the current cell at time t, where a_t and C_t are recurrently employed as the inputs of the next memory block[3]. Note that the last sigmoid function in the upper right corner is only included in the last cell of the LSTM network, and is used to produce the network output $\hat{y}_{t+1}$ in $[0, 1]$.
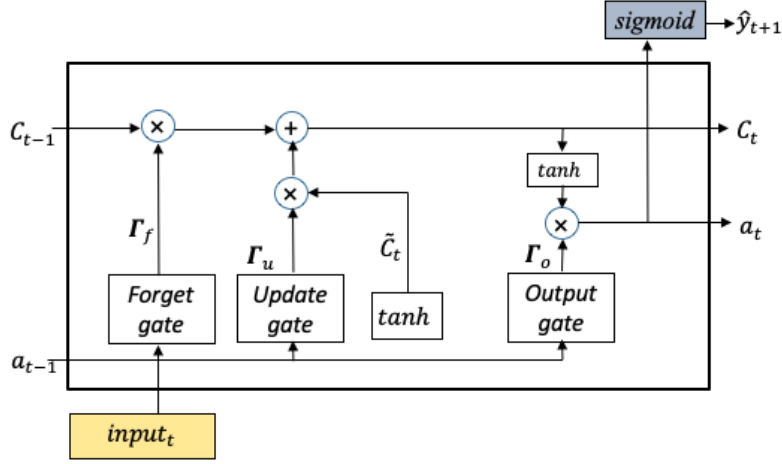

Figure 1: The LSTM cell inner structure at time t.

For each cell of LSTM, the formulae of the three gates, $\mathbf{\Gamma}_f, \mathbf{\Gamma}_u, \mathbf{\Gamma}_o$ and the new candidate state $\tilde{C}_t$ can be written as:

$$\mathbf{\Gamma}_f = \sigma(x_t U^f + a_{t-1} W^f);$$
$$\mathbf{\Gamma}_u = \sigma(x_t U^u + a_{t-1} W^u);$$
$$\mathbf{\Gamma}_o = \sigma(x_t U^o + a_{t-1} W^o);$$
$$\tilde{C}_t = tanh(x_t U^g + a_{t-1} W^g)$$

where σ is the sigmoid function, x_t is the input vector, a_t is the activation, U is the weighted matrix connecting inputs to the current layer, W is the recurrent connection between the previous and current layers. Therefore, $\mathbf{\Gamma}_{f,u,o}$ implies the level of information that each gate processes after balancing between the previous activation and the current input. The candidate state $\tilde{C}_t$ is computed based on the current input and the previous hidden state, and later added to the next cell state C_t on the basis of C_{t-1}.

This study applies LSTM as the predictive model and infers stock market turmoils on daily basis using historical information of a fixed window size l. As Figure 2 shows, each prediction is made from a network of l LSTM memory blocks that sequentially process the input of both the explanatory variables $\{\boldsymbol{x}_{t-l+1}, ..., \boldsymbol{x}_t\}$ and the SWARCH filtering

---
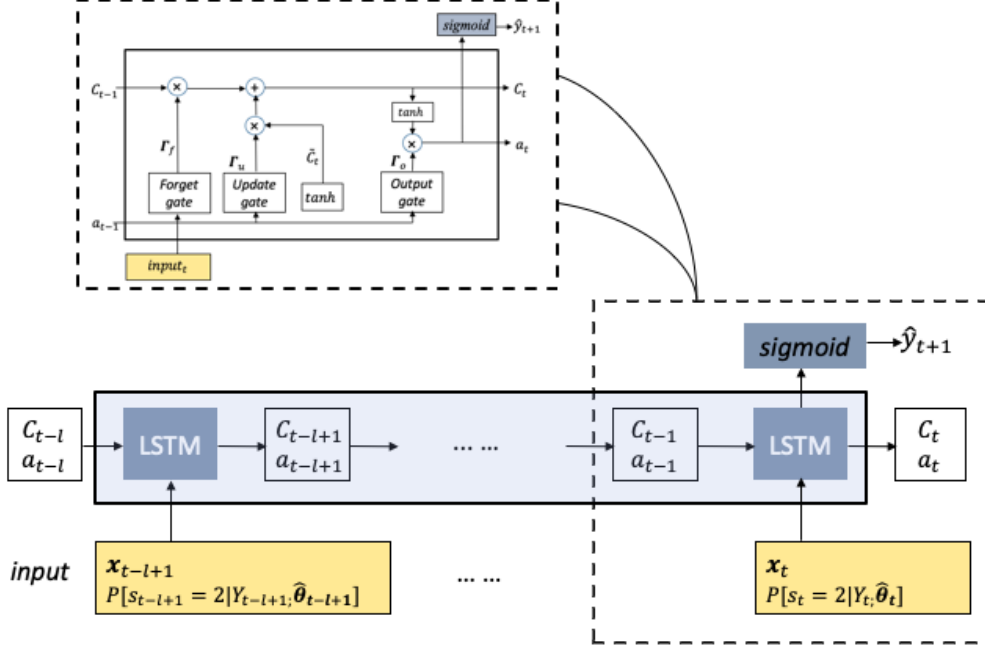
[3]The initial values of C_0 and a_0 are both zero.

Figure 2: LSTM with window size l. The LSTM cell structure in Fig. 1 is the last cell of the window.

probability $\{P[s_{t-l+1} = 2|Y_{t-l+1}; \hat{\boldsymbol{\theta}}_{t-l+1}],...,P[s_t = 2|Y_t; \hat{\boldsymbol{\theta}}_t]\}$ from time $t - l + 1$ to t, for $t \geq l$. The output $\hat{y}_{t+1}$ is produced by a sigmoid function indicating the probability of high-volatility at $t + 1$. Early warning signals are thus released for time $t + 1$ once the value of $\hat{y}_{t+1}$ exceeds the two-peak threshold at t (See Section 3.1.2). The LSTM network consists of 13 input layers (the number of the input variables), 32 LSTM layers and the output layer, which brings 5921 parameters to be trained. The batch size and epoch number are 20 and 100, respectively. Given the sample size of T days, $T - l$ predictions will be made from $t = l + 1$ onward.

Figure 3 structures the integrated EWS regarding to its three key components, i.e. the crisis classifier, crisis predictor and warning generator. Specifically, the crisis classifier identifies stock market turmoils according to Eq. 5 based on the SWARCH filtering probability and the crisis cutoff determined by the two-peak method. The output of the crisis classifier then becomes the target variable and is fed into the LSTM crisis predictor together with other explanatory variables. Finally, early warning signals are generated as the predicted output exceeds the crisis cutoff. To make robust daily predictions, the system is performed on a dynamically-recursive basis. The procedure is described by Algorithm 1 on the sample of size T.

4. System evaluation

In this section, a comprehensive evaluation is conducted by studying first the crisis classifier and predictor (see Figure 2) separately, then the early warning system as a
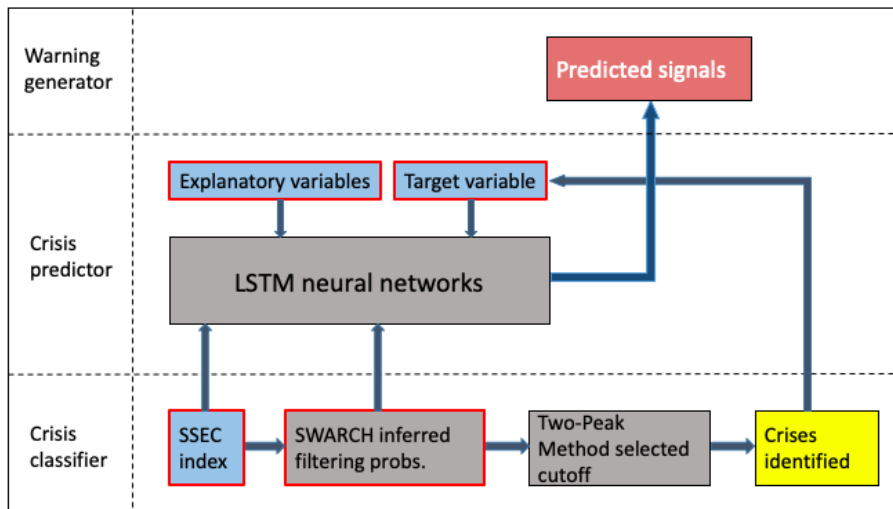
Figure 3: The structure of EWS with the crisis classifier, crisis predictor and the warning generator.

whole. In the view of the crisis classifier that jointly uses the SWARCH and two-peak method, we intend to understand its precision and robustness with empirical evidences. Next, the LSTM predictor is evaluated with two baselines, i.e. the back-propagation neural network (BPNN) and support vector regression (SVR), according to the performance metrics consisting of the rand accuracy (Rand, 1971), binary cross-entropy loss (Shannon, 1948), receiver operating curve (ROC), area under curve (AUC)(Metz, 1978) and the SAR score (Caruana and Niculescu-Mizil, 2004). Last, the early warning power of the entire system is investigated according to its test-set performance, cross-validation as well as back-testing.

4.1. Evaluating the crisis classifier

The credibility of an EWS is rooted in a precise and robust crisis classifier. According to Figure 2 and Algorithm 1, stock crisis cutoffs are computed dynamically for each prediction taking into account the current market condition as well as past information. To validate the reliability of the proposed classification mechanism, we analyze the crisis identification results in terms of its precision and robustness.

As crisis classification is a subjective topic heavily depending on the individual understanding of crisis, limited analysis could be done on quantitatively evaluating the accuracy due to the lack of true crisis labels. Given the target of the proposed EWS is to predict stock market turbulence, we investigate the precision of the crisis classifier with emphasis on the empirical evidence related to volatility regimes. Figure 4 and Table 3 summarizes the turmoils classified in the Chinese stock market by performing Algorithm 1 on the full sample. In Figure 4, crisis periods are highlighted in both the log return (grey in the upper panel) and filtering probability plots (red in the lower panel). As Figure 4 suggests, the proposed hybrid algorithm captures all the recorded stock crises that are also reflected by volatile log return and filtering probability jumps. Table 3 lists the starting and ending days of the detected turmoils with their associated critical

---
Algorithm 1: Daily warning for Chinese stock turbulence

 Initial inputs:
 　　　　The SSEC index price P_t;
 　　　　The explanatory variables $\boldsymbol{x}_t$ excluding P_t;
 Final output :
 　　　　The predicted signals $\hat{y}_{t+1}$;

1 calculate log returns of SSEC index price, $\{logR_t, t = 1, ..., T\}$;
2 set up the window size l;
3 **for** t *from* l *to* T **do**
4　　**repeat**
5　　　　**for** i *from* 1 *to* $t + 1$ **do**
6　　　　　　input $logR_i$ into SWARCH;
7　　　　　　output filtering probability $P[s_i = 2|Y_i; \hat{\boldsymbol{\theta}}_i]$;
8　　　　**end**
9　　　　two-peak method selects the optimal cutoff c_t;
10　　　　**for** i *from* 1 *to* $t + 1$ **do**
11　　　　　　**if** $P[s_i = 2|Y_i; \hat{\boldsymbol{\theta}}_i] \geq c_t$ **then**
12　　　　　　　　$\text{Crisis}_i = 1$;
13　　　　　　**end**
14　　　　**end**
15　　　　**for** j *from* 1 *to* l **do**
16　　　　　　input explanatory variable vector $\boldsymbol{x}_{t-l+j}$, filtering probability
 　　　　　　　$P[s_{t-l+j} = 2|Y_{t-l+j}; \hat{\boldsymbol{\theta}}_{t-l+j}]$ and identified crisis signals Crisis_{t-l+j}
 　　　　　　　into LSTM;
17　　　　**end**
18　　　　output the prediction $\hat{y}_{t+1}$;
19　　**until** $t{=}T$;
20 **end**

---

events. The hybrid classifier identifies crises with promising results explaining not only major global turmoils including the 2008 global financial crisis and 2010 European debt crisis, but also local stock turbulence resulted from the industrial reformation in 2013, the high-leveraging bubble collapse in 2015 and the economic slowdown since 2018.

The robustness of a model broadly refers to its error-resisting strength and resilience in producing results as data changes. Therefore, robust crisis classifications are subject to a dynamical thresholding mechanism to handle turbulence with limited influence from sample variations. Table 4 summarizes the statistics of crisis cutoffs that are determined in the full sample and test set by Algorithm 1. The number of cutoffs in a sample is given by the difference between the number of observations T and the window size l. With windows of size 5 (days), this study computes 2430 and 725 cutoffs in the full sample and test set of lengths 2434 and 729 (days), respectively. As Table 4 displays, the cutoff distributions of the full sample and test set are both right skewed given the greater means (0.515, 0.429) than the medians (0.489, 0.396) and modes (0.483, 0.355). In other words, the positive skewness indicates that cutoffs are more likely to take values below
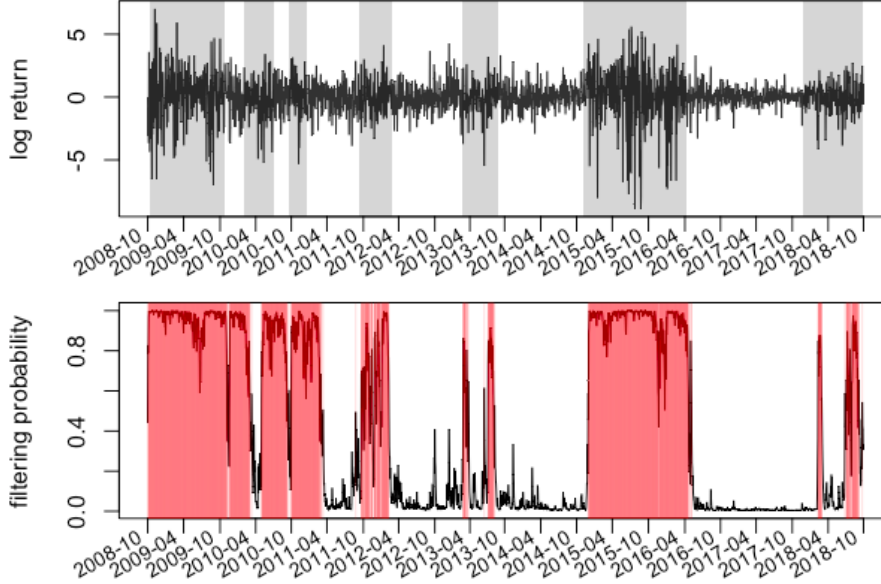
Figure 4: Log return of the SSEC stock index (upper panel) and the corresponding high-volatility filtering probability (lower panel). Turmoil periods determined by Algorithm 1 are highlighted in grey and red.

Table 3: Turmoil periods that are identified by Algorithm 1 in the full sample and associated critical events.

Event	Identified Crisis Period
2008 Global financial crisis	2008/10/04 - 2009/11/06
	2009/11/16 - 2010/03/28
2010 European debt crisis	2010/05/06 - 2010/09/16
	2010/10/08 - 2011/03/17
	2011/09/22 - 2012/02/17
2013 Industrial reformation	2013/03/04 - 2013/08/12
2015 Chinese stock crash	2014/12/02 - 2016/04/27
	2016/05/09 - 2016/05/11
2018 Domestic economy slowdown	2018/02/09 - 2018/03/06
	2018/07/02 - 2018/08/03
	2018/08/06 - 2018/08/31
	2018/09/04 - 2018/09/26

the mean and around the median/mode. Moreover, test-set cutoffs exhibit lower values with mean, median and mode approximating to 0.4, whereas those in the full sample are closer to 0.5. To explain this difference in the crisis cutoff distributions, Figure 5 shows the smoothed histograms of SWARCH filtering probabilities in the full (upper panel) and test (lower panel) sets. The optimal cutoffs determined at the end of Algorithm 1 for the last day observation are circled in blue. Although the test set exhibits a greater proportion of tranquil days with a significantly higher right peak, the two-peak method detects the true valley at 0.35 to threshold the crisis.

11

Table 4: Statistics of crisis cutoffs in the full sample and test set.

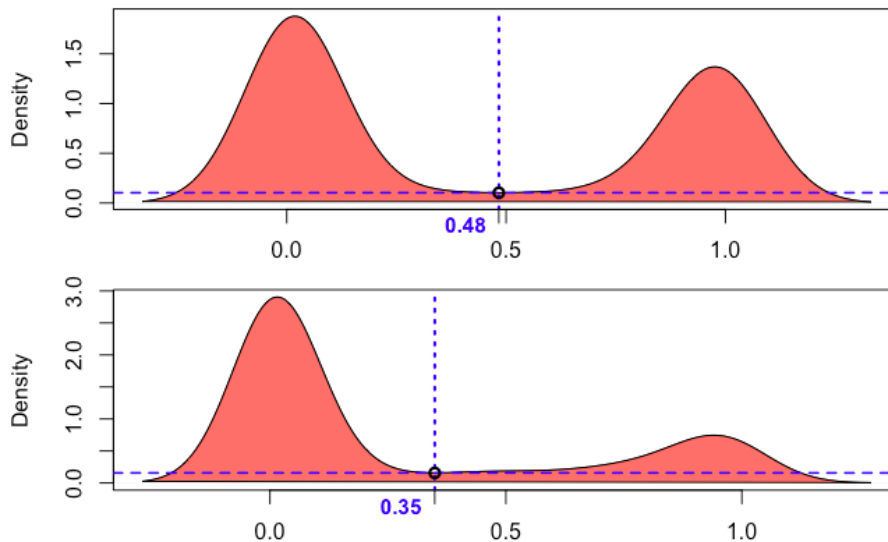|	Count	Mean	St.Dev	Median	Mode	Range
$\text{Cutoff}_{\text{full-sample}}$	2430	0.515	0.128	0.489	0.483	1.00
$\text{Cutoff}_{\text{test-set}}$	725	0.429	0.121	0.396	0.355	0.996

Figure 5: Cutoffs selected by the two-peak method in the full sample (upper panel) and test set (lower panel).

Further with the argument that a robust classification model ought to produce stable classification results regardless of the sampled information, Table 5 compares stock crises identified by Algorithm 1 with those defined on the CMAX indicator[4]. Daily classifications are computed in both the full-sample and test set for each model. To examine the level of consistency between crises identified on different samples, Table 5 lists the number (Row 3) and percentage (Row 5) of days that the full-sample crises differ from the test-set crises during the period from 2015/10/13 to 2018/09/28 (729 days in total)[5]. With 16 days of deviation in a period of almost three years and a percentage of 2.19%[6], the integrated EWS produces the most robust crisis classification result in comparison to the CMAX indicator on a range of parameters $\lambda = 1, 1.5, 2, 2.5$.

---

[4]The CMAX index is the most widely used crisis indicator in the literature concerning stock market early warning (Coudert and Gex, 2008; Li et al., 2015; Fu et al., 2019). It defines stock crashes with an indicator function $1_{CMAX_t < \mu_t - \lambda\sigma_t} CMAX_t : 1$, where μ_t and σ_t are the mean and standard deviation of $CMAX_t$, and λ is a market-dependent constant (Kaminsky and Reinhart, 1999). In this study, we consider four cases when $\lambda = 1, 1.5, 2, 2.5$ as they give reasonable results for Chinese stock market crises.

[5]This is the period when full sample and test set intersect.

[6]We believe that the percentage deviation of 2.19% could be further reduced with a larger sample of test set and cross validation. Relevant analyses on this aspect will be conducted in the future study.

Table 5: Difference between crises identified on the full sample and test set during 2015/10/13 - 2018/09/28.

	Integrated EWS	CMAX$_{\lambda=1}$	CMAX$_{\lambda=1.5}$	CMAX$_{\lambda=2}$	CMAX$_{\lambda=2.5}$
No. of crises with full sample	191	203	148	3	0
No. of crises with test set	207	154	112	115	67
No. of non-matching days	**16**	49	36	112	67
Total no. of days	729	729	729	729	729
% of non-matching days	**2.19**	6.27	4.94	15.4	9.19

4.2. Evaluating the crisis predictor

We now evaluate the crisis predictor based on LSTM in comparison to two baselines of BPNN and SVR. The associated performance metrics is discussed in Section 4.2.1. And Section 4.2.2 presents the results.

4.2.1. Evaluation metrics

The evaluation metrics of the predictor include three classes of performance measures that are designed for classification models, i.e. (I) the rand accuracy (Rand, 1971) and binary cross-entropy loss (Shannon, 1948), (II) the receiver operating curve (ROC) and area under curve (AUC) (Metz, 1978), and (III) the SAR score (Caruana and Niculescu-Mizil, 2004). Prior to the performance evaluation, Table 6 lists the confusion matrix that is used by the rand accuracy, ROC and SAR score.

Table 6: Confusion matrix for daily stock early warning.

Actual/Predicted	1: Crisis	0: Non-crisis
1: Crisis	True positive (TP)	False negative (FN)
0: Non-crisis	False positive (FP)	True negative (TN)

In general, true positive/negative corresponds to the true prediction of turmoil/tranquility, whereas false positive/negative corresponds to the false prediction. Moreover, the true positive rate (TPR) and false positive rate (FPR) are defined as the percentage of truly predicted crisis signals over the total number of actual crises, and the percentage of falsely predicted crisis signals over the total number of actual tranquility, respectively.

$$\text{TPR} = \frac{\text{TP}}{\text{TP} + \text{FN}}, \quad \text{FPR} = \frac{\text{FP}}{\text{FP} + \text{TN}}. \tag{6}$$

Evaluation Metric I: The rand accuracy is defined as the proportion of true results over the total number of cases examined:

$$\text{Accuracy} = \frac{\text{TP} + \text{TN}}{\text{TP} + \text{TN} + \text{FP} + \text{FN}}. \tag{7}$$

The binary cross-entropy loss measures the performance of classification models in terms of the level that the predicted probability of getting 1 deviates from the true label 0 or 1, and is expressed as:

$$\text{Loss} = -\frac{\sum_{i=1}^{n-l+1}(y_i log(\hat{y}_i) + (1 - y_i)log(1 - \hat{y}_i))}{n - l + 1}, \tag{8}$$

where y_i and $\hat{y}_i$ denote the true and predicted values, and n is the sample size. As we set the label of crises to be $True$ $(= 1)$, an EWS model that warns all the crises regardless the number of $False$ alarms it creates, has zero loss indicating none of the crisis is lost. According to Eq. (7) and (8), a greater level of predictive power comes along with higher rand accuracy and lower binary cross-entropy loss.

Evaluation Metric II: As one of the most classic performance measures, ROC plots the FPR (x-axis) against the TPR (y-axis) for each classifier. As a higher true positive rate is always more preferable given the level of the false positive rate, models with the ROC curve bending closer towards the upper-left corner are more preferable. To offer a quantitative representation of the graphic information carried by ROC, AUC computes the total area under the ROC curve and suggests the better model with the greater AUC value.

Evaluation Metric III: Different from the widely-used F1-score, the SAR score (Caruana and Niculescu-Mizil, 2004) is developed as a more holistic performance measure due to the uncertainty of the correct evaluation metric. By taking into account three distinctive measures including the accuracy, AUC and root mean-squared error (RMSE), models with higher SARs are regarded as better-performing as they produce overall high accuracy/AUC and low RMSE.

$$\text{SAR} = \frac{1}{3}(\text{Accuracy} + \text{AUC} + (1 - \text{RMSE})). \tag{9}$$

4.2.2. Test-set performance

To evaluate the predictive power of LSTM, BPNN and SVR, Table 7 preliminarily lists the test-set rand accuracy and binary cross-entropy loss of the three models following Algorithm 1[7]. Three window sizes $l = 22, 10, 5$ are considered. As Table 7 suggests, LSTM with window size $l = 5$ produces the optimal crisis prediction that yields the highest accuracy 0.952 and lowest loss 0.27 among all cases examined. Among the three predictive models, LSTM consistently demonstrates the strongest forecasting power of stock crises given different window sizes. Moreover, it is observed that with the last five days of information, all the three models achieve the best result (except the accuracy of SVR) in comparison to the predictions made with 22 and 10 days information. Therefore, the remaining of the evaluation is conducted with window size 5.

Figure 6 further shows the test-set ROC and SAR curves. In particular, Panel (a) shows the ROC curves and AUC values generated from the test-set predictions. As the ROC-oriented metric tells the model's ability in classifying the binary states, LSTM enhances BPNN and SVR with its outstanding capacity in distinguishing turbulence/tranquility with the optimal ROC curve and AUC value of 0.997.

Panel (b-d) plot the SAR score against the crisis cutoff for the three predictive models. According to Algorithm 1, the test-set score of each model is highlighted as the blue point in each panel corresponding to the last day cutoff obtained from the dynamic crisis

---

[7]To obtain the baseline results, Algorithm 1 is implemented by replacing the LSTM in line 16 by BPNN and SVR.

Table 7: Test-set rand accuracy and binary cross-entropy loss based on LSTM, BPNN and SVR with varying the window sizes

	LSTM	BPNN	SVR
Window size $l = 22$			
Accuracy	0.930	0.882	0.927
Binary cross-entropy loss	0.380	0.439	0.407
Window size $l = 10$			
Accuracy	0.941	0.865	0.920
Binary cross-entropy loss	0.326	0.305	0.405
Window size $l = 5$			
Accuracy	**0.952**	0.899	0.912
Binary cross-entropy loss	**0.270**	0.369	0.423

classifier, whereas the red point is the highest score obtained by the predictive model regardless of the optimal cutoff. From the perspective of model scores, LSTM remains its dominating state with the highest test-set score (blue) of 0.9, whereas BPNN and SVR score 0.74 and 0.77, respectively. Moreover, LSTM appears to be the most insensitive model to cutoff variations as the scores remain relatively high in a prolonged range shaped as a flat peak in Panel (b). With a similar shape in Panel (c), BPNN produces a SAR curve with reduced scores and a smaller peak, where the test-set score 0.74 exhibits a large deviation from the best score of 0.86. Despite that SVR produces close scores as BPNN, the sharp peak in Panel (d) suggests the model's instability in predicting with varying cutoffs.
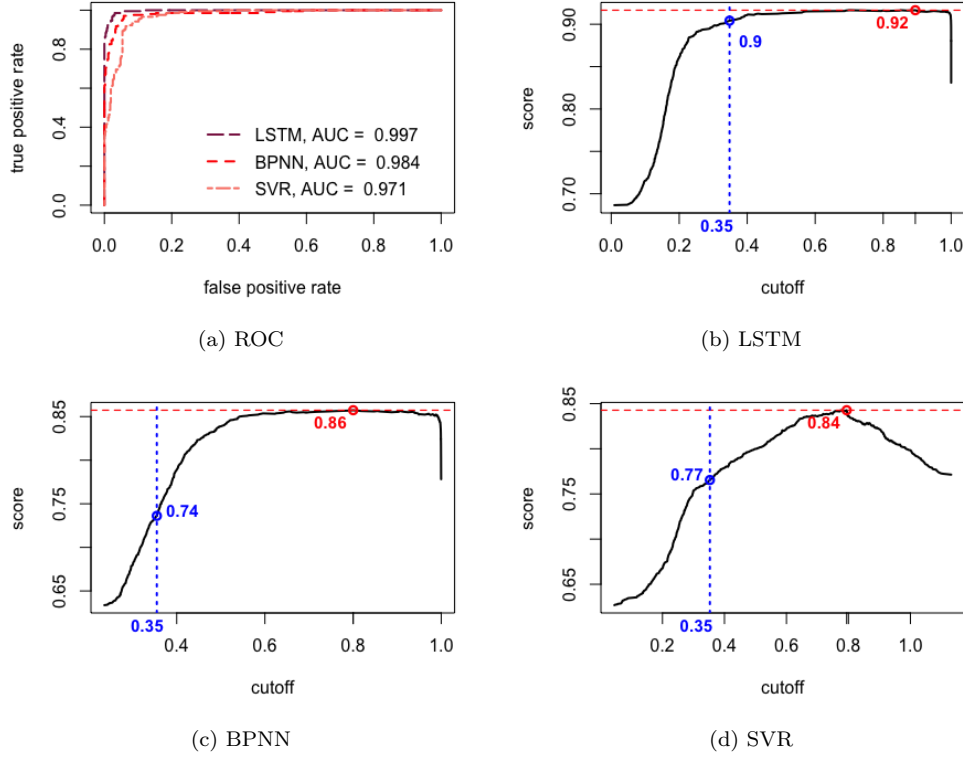
15

(a) ROC (b) LSTM

(c) BPNN (d) SVR

Figure 6: Test-set ROC (Panel a) and SAR (Panel b-d) curves of LSTM, BPNN and SVR.

4.3. Crisis early warning

In this section, we examine the integrated EWS in terms of its early warning power with respect to the forewarned period ahead of the actual crisis onsets. By keeping BPNN and SVR as baselines, test-set forecasting, cross-validation and back-testing are implemented. In this way, we hope to gain a comprehensive understanding on the system's crisis forecasting capacity, stability as well as effectiveness.

4.3.1. Test-set performance

Figure 7 shows the predicted signals by the integrated EWS against their true crisis labels (1 for crisis and 0 otherwise) by the SWARCH model. As Figure 7 displays, crisis onsets in the test set mainly occur in 2016 as a result of the lasting effect from the 2015 stock market crash, and in 2018 due to the financial instability in China. Overall, the proposed EWS with LSTM predictions depict the test-set set crises in a relatively precise manner with the first alarms (red line) before the actual onsets (blue dashed line). As the predictive model is replaced by BPNN, the EWS tends to delay in producing the first crisis signal despite of its ability in capturing ongoing crises. In contrast to LSTM and BPNN, SVR appears to suffer from both delayed warnings and false alarms in Figure 7.
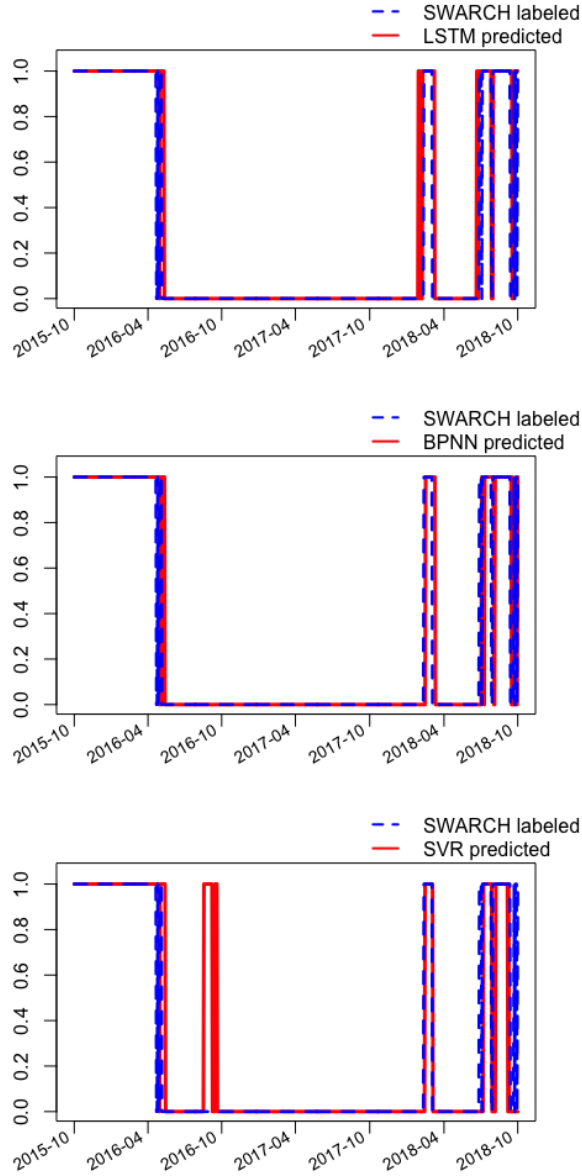
16

Figure 7: Test-set early warning signals

To support the preceding claims with evidence, Table 8 summarizes the numerical results related to the test-set forecasting. The test set consists of 729 days with 207 crisis days (Row 2, Table 8) and 6 crisis onsets (Row 6, Table 8). With respect to Table 8, EWS with LSTM demonstrates a promising capability of warning stock turbulence that is reflected by its dominating results in all aspects examined. In particular, LSTM-based

17

EWS improves the baselines with 200 days of correct predictions which yield a rate of 96.6%. On average, the model alerts stock turbulence 2.4 days ahead of the actual crises and successfully warns 83.3% of the onsets with 0% false alarm. It is worth-mentioning that the missed onset occurs two days after its preceding crisis on July 25, 2018 and lasts for one day only. In line with the observations made from Figure 7, the major weakness of the BPNN-based EWS reveals due to its delay in generating crisis signals, which is suggested by a relatively high rate of correct daily predictions 94.6% and a low rate of successfully predicted onsets 33.3%. Beside the delays, the high percentage of 30% false alarms makes SVR the least reliable model for the early warning task in comparison to LSTM and BPNN.

Table 8: Summary of test-set forecasting. % of correct predictions is the percentage of correctly predicted crisis signals, % of correct predicted onsets is the percentage of correctly forewarned onsets.

Model	LSTM	BPNN	SVR
Total crises	207	207	207
Correct predictions	**200**	196	184
% of correct predictions	**96.6**	94.6	88.9
Total onsets	6	6	6
Predicted onsets	**5**	2	2
% of correct predicted onsets	**83.3**	33.3	33.3
% of false onset alarms	0.0	0.0	30.0
Avg. days-ahead onsets	**2.4**	1.5	2.0

4.3.2. Cross validation

To analyze the stability of the EWS, a k-fold cross validation is further conducted in the test set with varying values $k = 3, 5, 8$[8]. Rand accuracy and cross-entropy loss are used as the performance measures.

The governing performance of the LSTM-based EWS is proven to be robust in the cross validation. Given different k values, LSTM invariably produces the greatest accuracy and lowest loss in comparison to the baselines. In particular, EWS with LSTM achieves the best test-set accuracy of 95.1% in the 5-fold validation. And even with 3-fold validation, LSTM obtains an accuracy of 91.9% and loss of 16.5% in the test set.

4.3.3. Back-testing

In the back-testing, a simple trading strategy is adopted to the SSEC stock index with the aim to verify the effectiveness of the proposed EWS from a practical perspective. Assuming symmetric information between the market and the investors with a fair level of risk aversion, a market portfolio of SSEC index is constructed and held until the EWS alerts crises, and repurchased as the EWS suggests tranquility. Table 10 summarizes the expectation and standard deviation of returns together with Sharp ratios in the full

---

[8]Given the selection of k deals with the trade-off between bias and variance, the cross validation is conducted up to 8 folds in order to ensure the size of the test set is large enough to offer statistically representative of the model's forecasting power.

Table 9: Average test-set rand accuracy and binary cross-entropy loss from the k-fold cross validation

	LSTM	BPNN	SVR
$k = 3$			
Accuracy (avg.)	0.919	0.896	0.909
Binary cross-entropy loss (avg.)	**0.165**	0.314	0.658
$k = 5$			
Accuracy (avg.)	**0.951**	0.911	0.923
Binary cross-entropy loss (avg.)	0.218	0.288	0.454
$k = 8$			
Accuracy (avg.)	0.913	0.858	0.884
Binary cross-entropy loss (avg.)	0.168	0.476	0.389

sample and test set. In the absence of early warning mechanisms, the market portfolio yields expected returns of 2.3% and -0.5% and standard deviations 1.48 and 1.156% in the full sample and test set, respectively. The corresponding Sharp ratios are 1.6% and -0.4%. By exiting the market position with respect to early warned turbulence, the strategy significantly reduces the systematic risk (indicated by the σ), which naturally results in a higher level of Sharp ratio, regardless of the predictive model.

More importantly, back-testing once more verifies that the LSTM-based EWS outperforms the baselines and holds the greatest effectiveness and stability. Specifically, the effectiveness of LSTM is proven by its dominating Sharp ratios which improve the market portfolio by 3.8% and 2.4% in the full sample and test set, respectively. Meanwhile, its stability is suggested by the monotonous positive impact on the market portfolio regarding to the three portfolio measures in the risk-return horizon. Albeit the moderate improvements achieved by BPNN (Sharp ratios 4.6% and 0.2% in the full sample and test set) and SVR (Sharp ratios -0.1% and 0.5%), the two models exhibit limitations due to their weaker and fluctuating results.

5. Conclusions

In this study, a novel EWS with a dynamic architecture integrating the SWARCH model, two-peak thresholding and LSTM is developed to identify and predict stock market turbulence. According to the models' performance on the ten-year sample of Shanghai Stock Exchange Composite index, the following concluding remarks are emerged.

1. As one of the most powerful models handling sequential data, LSTM remains its outstanding position in the daily prediction task of stock crises. To be specific, the reliability of LSTM in this study is not only reflected by the high accuracy of 96.6% and on average 2.4 days of forewarned period, but also its stability of outperforming the baselines throughout the evaluation process in the test-set, cross-validation as well as back-testing.

Table 10: Back-testing in the full sample and test set. $E[R_p]$ is the expected return rate, σ_p is the standard deviation and $SharpeRatio$ is given by $SharpeRatio = \frac{E[R_p]-R_f}{\sigma_p}$, where R_f denotes the risk free interest rate and is set to zero in our study.

	$E[R_p]$	σ_p	$SharpeRatio$
full-sample			
market portfolio	0.023	1.480	0.016
EWS-LSTM	0.039	0.718	**0.054**
EWS-BPNN	0.045	0.983	0.046
EWS-SVR	-0.001	0.687	-0.001
test set			
market portfolio	-0.005	1.156	-0.004
EWS-LSTM	0.012	0.610	**0.020**
EWS-BPNN	0.004	0.625	0.002
EWS-SVR	0.003	0.594	0.005

2. In addition to a high-performing predictive model, a precise and robust crisis identification mechanism also plays the central role in facilitating the effectiveness and reliability of an EWS. By adopting the two-peak method to determine crisis cutoffs, the proposed EWS suggests a constructive alternative to current existing approaches, and yields promising crisis classifications in the Chinese stock market in comparison to the classic indicator function based on CMAX.

3. Stock market turbulence described by the SWARCH volatility regimes is proven to be a good crisis indicator in both theory and practice, as the proposed EWS depicts all the recorded major stock crises in the sample with significantly improved back-testing results than the market portfolio.

For future study, we plan to further investigate the proposed EWS structure in terms of other crisis thresholding and prediction mechanisms. At the same time, we are interested in applying the integrated EWS to predict other types of financial crises, e.g. currency or banking crises, in different frequency domains.

Acknowledgement

References

Ahn, J.J., Oh, K.J., Kim, T.Y., Kim, D.H., 2011. Usefulness of support vector machine to develop an early warning system for financial crisis. Expert Systems with Applications 38, 2966–2973.

Babecký, J., Havránek, T., Matějů, J., Rusnák, M., Šmídková, K., Vašiček, B., 2014. Banking, debt, and currency crises in developed countries: Stylized facts and early warning indicators. Journal of Financial Stability 15, 1–17.

Beckmann, R., 2007. Profitability of Western European banking systems: panel evidence on structural and cyclical determinants. Discussion Paper Series 2: Banking and Financial Studies 2007,17. Deutsche Bundesbank. URL: `https://ideas.repec.org/p/zbw/bubdp2/6929.html`.

BenMim, I., BenSaïda, A., 2019. Financial contagion across major stock markets: A study during crisis episodes. The North American Journal of Economics and Finance 48, 187–201.

BenSaïda, A., 2018. The contagion effect in European sovereign debt markets: A regime-switching vine copula approach. International Review of Financial Analysis 58, 153–165. doi:`10.1016/j.irfa.2017.10.00`.

Berg, A., Pattillo, C., 1999. Predicting currency crises: The indicators approach and an alternative. Journal of international Money and Finance 18, 561–586.

Bussiere, M., Fratzscher, M., 2006. Towards a new early warning system of financial crises. journal of International Money and Finance 25, 953–973.

Cao, J., Li, Z., Li, J., 2019. Financial time series forecasting model based on ceemdan and lstm. Physica A: Statistical Mechanics and its Applications 519, 127–139.

Caprio, G., Klingebiel, D., 2002. Episodes of systemic and borderline banking crises. Managing the real and fiscal effects of banking crises, World Bank Discussion Paper 428, 31–49.

Caruana, R., Niculescu-Mizil, A., 2004. Data mining in metric space: an empirical analysis of supervised learning performance criteria, in: Proceedings of the tenth ACM SIGKDD international conference on Knowledge discovery and data mining, ACM. pp. 69–78.

Celik, A.E., Karatepe, Y., 2007. Evaluating and forecasting banking crises through neural network models: An application for turkish banking sector. Expert Systems with Applications 33, 809 – 815. URL: `http://www.sciencedirect.com/science/article/pii/S0957417406002132`, doi:`https://doi.org/10.1016/j.eswa.2006.07.005`.

Chen, K., Zhou, Y., Dai, F., 2015. A lstm-based method for stock returns prediction: A case study of china stock market, in: 2015 IEEE International Conference on Big Data (Big Data), IEEE. pp. 2823–2824.

Coudert, V., Gex, M., 2008. Does risk aversion drive financial crises? testing the predictive power of empirical indicators. Journal of Empirical Finance 15, 167–184.

Davis, E.P., Karim, D., 2008. Comparing early warning systems for banking crises. Journal of Financial Stability 4, 89 – 120. URL: `http://www.sciencedirect.com/science/article/pii/S1572308908000144`, doi:`https://doi.org/10.1016/j.jfs.2007.12.004`.

Demirg-Kunt, A., Detragiache, E., 1998. The determinants of banking crises in developing and developed countries. Staff Papers (International Monetary Fund) 45, 81–109. URL: `http://www.jstor.org/stable/3867330`.

Detragiache, M.E., Spilimbergo, M.A., 2001. Crises and liquidity: evidence and interpretation. 1-2, International Monetary Fund.

Duan, P., Bajona, C., 2008. China's vulnerability to currency crisis: A klr signals approach. China Economic Review 19, 138–151.

Edison, H.J., 2003. Do indicators of financial crises work? an evaluation of an early warning system. International Journal of Finance & Economics 8, 11–53.

Edwards, S., Susmel, R., 2001. Volatility Dependence and Contagion in Emerging Equity Markets. Journal of Development Economics 66, 505–532. URL: `https://ideas.repec.org/a/eee/deveco/v66y2001i2p505-532.html`.

Eichengreen, B., Rose, A.K., 1998. Staying Afloat When the Wind Shifts: External Factors and Emerging-Market Banking Crises. Working Paper 6370. National Bureau of Economic Research. URL: `http://www.nber.org/papers/w6370`, doi:`10.3386/w6370`.

Eichengreen, B., Rose, A.K., Wyplosz, C., 1995. Exchange market mayhem: the antecedents and aftermath of speculative attacks. Economic policy 10, 249–312.

Fang, H., 2012. Adaptive neurofuzzy inference system in the application of the financial crisis forecast. International Journal of Innovation, Management and Technology 3, 250.

Fink, H., Klimova, Y., Czado, C., Stober, J., 2016. Regime switching vine copula models for global equity and volatility indices. Econometrics 5. doi:`10.3390/econometrics5010003`.

Fischer, T., Krauss, C., 2018. Deep learning with long short-term memory networks for financial market predictions. European Journal of Operational Research 270, 654–669.

Frankel, J.A., Rose, A.K., 1996. Currency crashes in emerging markets: An empirical treatment. Journal of International Economics 41, 351 – 366. URL: `http://www.sciencedirect.com/`

science/article/pii/S0022199696014419, doi:https://doi.org/10.1016/S0022-1996(96)01441-9. symposium on Mexico.

Fu, J., Zhou, Q., Liu, Y., Wu, X., 2019. Predicting stock market crises using daily stock market valuation and investor sentiment indicators. The North American Journal of Economics and Finance .

Giovanis, E., 2012. Study of discrete choice models and adaptive neuro-fuzzy inference system in the prediction of economic crisis periods in usa. Economic Analysis and Policy 42, 79–96.

Hamilton, J., Gang, L., 1996. Stock Market Volatility and the Business Cycle. Journal of Applied Econometrics 11, 573–93. URL: https://EconPapers.repec.org/RePEc:jae:japmet:v:11:y:1996:i:5:p:573-93.

Hamilton, J.D., Susmel, R., 1994. Autoregressive conditional heteroskedasticity and changes in regime. Journal of Econometrics 64, 307 – 333. URL: http://www.sciencedirect.com/science/article/pii/0304407694900671, doi:https://doi.org/10.1016/0304-4076(94)90067-1.

Hochreiter, S., Schmidhuber, J., 1997. Long short-term memory. Neural Comput. 9, 1735–1780. URL: http://dx.doi.org/10.1162/neco.1997.9.8.1735, doi:10.1162/neco.1997.9.8.1735.

Hu, Y., Pang, J., 2008. Financial crisis early-warning based on support vector machine, in: 2008 IEEE International Joint Conference on Neural Networks (IEEE World Congress on Computational Intelligence), IEEE. pp. 2435–2440.

Hui, S.b., Wang, W.j., . Research of financial early-warning model based on support vector machine. Computer Engineering and Design 7.

Jain, R., Kasturi, R., Schunck, B.G., 1995. Machine vision. volume 5. McGraw-Hill New York.

Jordan, M., 1997. Serial order: A parallel distributed processing approach. Advances in Psychology 121, 471–495. doi:10.1016/S0166-4115(97)80111-2.

Kaminsky, G.L., 1998. Currency and banking crises: the early warnings of distress. Technical Report.

Kaminsky, G.L., 2006. Currency crises: Are they all the same? Journal of International Money and Finance 25, 503–527.

Kaminsky, G.L., Reinhart, C.M., 1999. The twin crises: The causes of banking and balance-of-payments problems. The American Economic Review 89, 473–500. URL: http://www.jstor.org/stable/117029.

Kibritcioglu, B., Kose, B., Ugur, G., 1999. A leading indicators approach to the predictability of currency crises: the case of turkey. Hazine Dergisi, Sayi Working Paper .

Kim, H.Y., Won, C.H., 2018. Forecasting the volatility of stock price index: A hybrid model integrating lstm with multiple garch-type models. Expert Systems with Applications 103, 25–37.

Kim, K., 2013. Modeling financial crisis period: A volatility perspective of credit default swap market. Physica A: Statistical Mechanics and its Applications 392, 4977–4988.

Kim, T.Y., Hwang, C., Lee, J., 2004a. Korean economic condition indicator using a neural network trained on the 1997 crisis. Journal of Data Science 2, 371–381.

Kim, T.Y., Oh, K.J., Sohn, I., Hwang, C., 2004b. Usefulness of artificial neural networks for early warning system of economic crisis. Expert Systems with Applications 26, 583–590.

Laeven, L., Valencia, F., 2012. Systemic banking crises database: An update .

Laeven, M.L., Valencia, F., 2010. Resolution of banking crises: The good, the bad, and the ugly. 10-146, International Monetary Fund.

Li, W.X., Chen, C.C.S., French, J.J., 2015. Toward an early warning system of financial crises: What can index futures and options tell us? The Quarterly Review of Economics and Finance 55, 87–99.

Lin, C.S., Khan, H. A., C.R.Y.W.Y.C., 2008. A new approach to modeling early warning systems for currency crises: Can a machine-learning fuzzy expert system predict the currency crises effectively? Journal of International Money and Finance 27, 1098–1121.

Liu, Y., 2019. Novel volatility forecasting using deep learning–long short term memory recurrent neural networks. Expert Systems with Applications 132, 99–109.

Metz, C.E., 1978. Basic principles of roc analysis. Seminars in Nuclear Medicine 8, 283 – 298. URL: http://www.sciencedirect.com/science/article/pii/S0001299878800142, doi:https://doi.org/10.1016/S0001-2998(78)80014-2.

Nag, A.K., Mitra, A., 1999. Neural networks and early warning indicators of currency crisis. In: Reserve Bank of India occasional papers.

Nan, G., Zhou, S., K.J.L.M., 2012. Heuristic bivariate forecasting model of multi-attribute fuzzy time series based on fuzzy clustering. International Journal of Information Technology and Decision Making 11, 167–195.

Oh, K.J., Kim, T.Y., Kim, C., 2006. An early warning system for detection of financial crisis using financial market volatility. Expert Systems 23, 83–98.

Ohtsu, N., 2007. A threshold selection method from gray-level histograms. IEEE Transactions on

Systems Man & Cybernetics 9, 62–66.

Prewitt, J., Mendelsohn, M., 1966. The analysis of cell images. Annals of the New York Academy of Sciences 128, 1035–53. doi:10.1111/j.1749-6632.1965.tb11715.x.

Ramchand, L., Susmel, R., 1998. Volatility and Cross Correlation across Major Stock Markets. Journal of Empirical Finance 5, 397–416. URL: https://EconPapers.repec.org/RePEc:eee:empfin:v:5:y:1998:i:4:p:397-416.

Rand, W.M., 1971. Objective criteria for the evaluation of clustering methods. Journal of the American Statistical Association 66, 846–850. URL: http://www.jstor.org/stable/2284239.

Reinhart, C.M., Rogoff, K.S., 2011. From financial crash to debt crisis. American Economic Review 101, 1676–1706.

Reinhart, C.M., Rogoff, K.S., 2013. Banking crises: an equal opportunity menace. Journal of Banking & Finance 37, 4557–4573.

Rodriguez, J.C., 2007. Measuring financial contagion: A copula approach. Journal of Empirical Finance 4, 401 – 423. URL: http://www.sciencedirect.com/science/article/pii/S0927539806000582, doi:https://doi.org/10.1016/j.jempfin.2006.07.002.

Rosenfeld, A., De La Torre, P., 1983. Histogram concavity analysis as an aid in threshold selection. IEEE Transactions on Systems, Man, and Cybernetics , 231–235.

Sevim, C., Oztekin, A., Bali, O., Gumus, S., Guresen, E., 2014. Developing an early warning system to predict currency crises. European Journal of Operational Research 237, 1095–1104.

Shannon, C.E., 1948. A mathematical theory of communication. Bell System Technical Journal 27, 623–656.

Valencia, F., Laeven, M.L., 2008. Systemic banking crises: A new database. 8-224, International Monetary Fund.

Wang, P., Zong, L., 2019. Contagion effects and risk transmission channels in the housing, stock, interest rate and currency markets: An empirical study in china and the u.s. (accepted). North American Journal of Economics and Finance .

Weszka, J.S., 1978. A survey of threshold selection techniques . Computer Graphics & Image Processing 7, 259–265.

Wu, Y., Gao, J., 2018. Adaboost-based long short-term memory ensemble learning approach for financial time series forecasting. Current Science (00113891) 115.

Yeyati, E.L., Panizza, U., 2011. The elusive costs of sovereign defaults. Journal of Development Economics 94, 95–105.

Yu, L., Wang, S., Lai, K.K., Wen, F., 2010. A multiscale neural network learning paradigm for financial crisis forecasting. Neurocomputing 73, 716–725.

Yu, S., Li, Z., 2018. Forecasting stock price index volatility with lstm deep neural network, in: Recent Developments in Data Science and Business Analytics. Springer, pp. 265–272.